

RESEARCH PAPER RP1110

*Part of Journal of Research of the National Bureau of Standards, Volume 21,
July 1938*

PRESSURE LOSSES FOR FLUID FLOW IN 90° PIPE BENDS

By K. Hilding Beij.

ABSTRACT

Pressure losses were determined for nine 4-inch steel, 90° pipe bends of radii from 6 to 80 inches. The results are discussed in relation to those found by previous investigators under comparable test conditions. For bends having radii of four pipe diameters or less, all the results which are discussed may be correlated on the basis of pipe roughness. Further data are needed to establish a working formula. No correlation could be obtained for the bends of larger radii. For such bends the maximum published values should be used in engineering work until more comprehensive data become available.

CONTENTS

	Page
I. Introduction	1
1. Purpose of work	1
2. Statement of problem	2
3. Previous work	3
II. Pipes and bends	3
III. Apparatus	4
IV. Experimental results	6
1. Resistance coefficients for straight pipe	6
2. Bend coefficients	8
3. Tangent coefficients	11
4. Deflection coefficients	14
V. Discussion of results	15
1. Rusting of pipes	15
2. Pipe joints	15
3. Bend coefficient	15
4. Tangent coefficient	18
5. Deflection coefficient	18
VI. Future work	18
VII. References	18

I. INTRODUCTION

1. PURPOSE OF WORK

The 90° pipe bend is perhaps the most frequently used fitting in piping systems. The pressure losses in such bends are therefore of considerable engineering importance. However, although many investigators have studied the problem, the results which they have obtained have not been satisfactorily correlated. The work discussed in this paper was undertaken to obtain information which would assist in the correlation of previous results, and further, to furnish data for engineering use. This work forms part of an extended study of pipe bends in progress at the National Hydraulic Laboratory, another part of which has already been published [1].¹

¹ Figures in brackets refer to the literature references at the end of this paper.

2. STATEMENT OF PROBLEM

In this paper the term *pipe bend* will be restricted to pipes of circular cross section bent to the form of circular arcs. A bend will always be considered with relation to the straight pipes connected to its two ends. These straight pipes, or *tangents*, are *long*; that is, whatever the velocity distribution may be at the upstream end, the length is sufficient for the gradual modification of the distribution until it assumes a characteristic form which remains unchanged for the remainder of the pipe. Thus, at the entrance to the bend the velocity distribution will be the characteristic distribution for straight pipe. At the downstream end of the bend the velocity distribution depends on the nature of the flow in the bend. This distribution changes gradually in the downstream tangent until it assumes the form characteristic of straight pipe. It is found that in the bend and in the downstream tangent, the pressure losses are greater than in equal lengths of straight pipe with characteristic velocity distribution.

The conventional manner of expressing the excess pressure losses in the bends and downstream tangents will be adopted. According to this view, we assume that the total loss in a bend with long tangents is the sum of the loss which would occur with characteristic velocity distribution in straight pipe of the same axial length, plus an excess loss in the bend, plus an excess loss in the downstream tangent. That is, measuring pressure losses between a point on the upstream and a point on the downstream tangent, at each of which characteristic velocity distribution for straight pipe prevails, we find

$$P/\gamma = H = H_s + H_B + H_T, \quad (1)$$

or putting

$$H_B = \xi \frac{U^2}{2g}, \quad (2)$$

$$H_T = \theta \frac{U^2}{2g}, \text{ and} \quad (3)$$

$$H_s = \lambda_s \frac{l}{d} \frac{U^2}{2g}, \quad (4)$$

we have

$$\frac{P}{\gamma} = H = \lambda_s \frac{l}{d} \frac{U^2}{2g} + \xi \frac{U^2}{2g} + \theta \frac{U^2}{2g}, \quad (5)$$

where

P =the total pressure loss,

γ =the specific weight of the fluid,

H =the total head loss (measured as the height of a column of the same fluid as that flowing in the pipe line),

H_s =the head loss with characteristic velocity distribution in a straight pipe of axial length equal to the distance between the points of pressure measurement,

H_B =the excess head loss in the bend,

H_T =the excess head loss in the downstream tangent,

U =the mean velocity, which is the quantity of flow, Q , divided by the cross-sectional area of the pipe, A ,

g =the acceleration of gravity,

λ_s =the coefficient of resistance for straight pipe with characteristic velocity distribution,

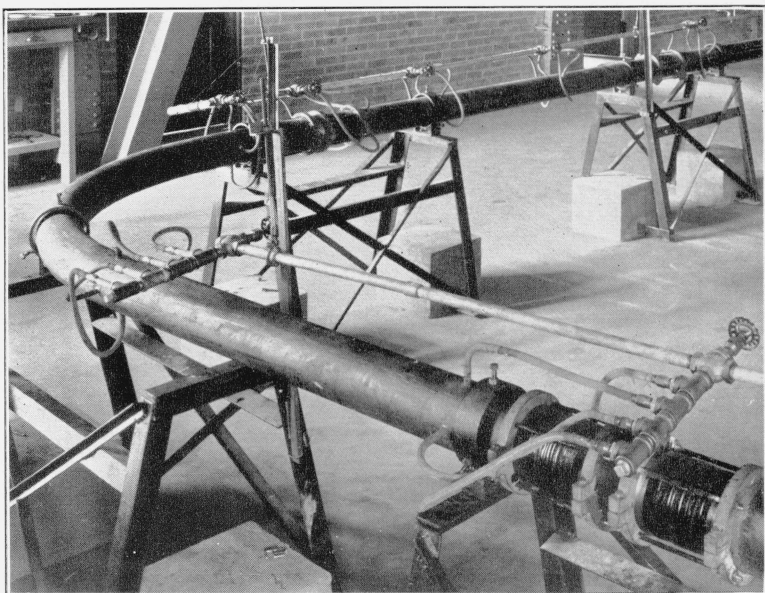


FIGURE 1.—*Pipe bend of long radius as set up for test.*

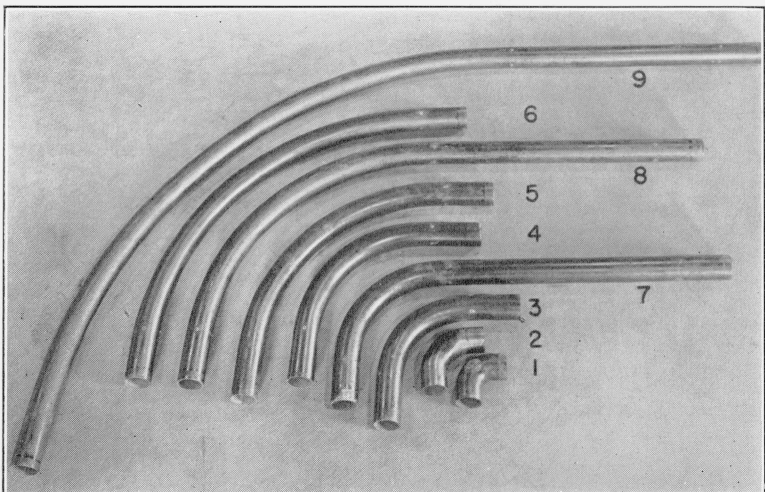


FIGURE 2.—*Pipe bends which were tested.*

l =the length of pipe,
 d =the diameter of the pipe,
 ξ =the deflection coefficient, and
 θ =the tangent coefficient.

We may also write

$$H = H_s + \eta \frac{U^2}{2g}, \quad (6)$$

where

$$\eta = \xi + \theta \quad (7)$$

is the bend coefficient.

It is tacitly assumed in these equations that the interior surfaces of the bend and the tangents are the same, the cross section does not vary, and no disturbing influences such as rough joints are present.

The coefficients η , ξ , and θ are, in general, functions of the dimensions and roughness of the pipe and bends, and the Reynolds number. The immediate problem is to determine these functions for 90° pipe bends.

3. PREVIOUS WORK

It is unnecessary to repeat here all previous results, since in many cases the published data are insufficient for the purpose of comparison, or the test conditions are not comparable with those of the present work. Therefore, only a few representative results have been selected either for direct comparison or to illustrate some particular point. See figures 8, 11, and 12. It must be emphasized that the results given in the figures represent the best which have been obtained, and that the discrepancies are far too large to be accounted for by experimental errors alone.

II. PIPES AND BENDS

Steel tubing of nominal 4-inch internal diameter, in lengths of 7 to 8 feet, was used. Internal diameters were measured with a pipe gage about 6 inches from each end of each pipe and on four diameters at about 45° spacing. The mean of all measurements was 10.23 cm and the maximum deviation from the mean was 0.03 cm.

At the joints the pipes were simply butted together and held in place by friction clamps around the pipe connected by bolts. The joint was made watertight by a wrapping of rubber tape laid in gasket shellac and covered by a layer of friction tape. To make the joints match perfectly, each pipe end was machined. The pipe was centered as truly as possible in a lathe, the end cut off square, and the outer surface machined back for a few inches from the end to a predetermined diameter. Finally, a finishing cut on a 0.5° taper (half-angle) was made on the inside until the inside diameter at the very end was a certain predetermined value. The change in diameter due to this tapering cut was in no case as great as 0.2 cm.

Similar joints were used on all the smaller bends. On those which were too large to be mounted in a lathe, a simplified joint was added. A piece about 9 inches long was cut from each end of the bend by a band saw, and matchmarked so that it could be returned to its original position. Burrs were removed by filing. The other end of each of these short pieces was then machined to match the straight pipe ends.

The joints which were made by sawing matched practically as well as those which were machined, but they were more difficult to assemble and to make watertight.

The pipes and bends were supported in clamping rings mounted on steel stands. The clamping screws were used to make final adjustments of the pipe to line and grade. Figure 1 shows one of the larger bends set up for test.

The bends are shown in figure 2. The two smallest (numbers 1 and 2) were standard seamless welding fittings to which short tangents were welded. The inside surfaces of the welds were ground true. All of the other bends were made of the same steel tubing as the straight pipes, bent to the desired dimensions. All had short integral tangents at both ends except three (numbers 7, 8, and 9) which had tangents approximately 4 feet long on the upstream ends.

III. APPARATUS

A diagram of the pipe line and the manometer connections is given in figure 3. A differential air-water manometer consisting of two glass tubes of about 23 mm bore was used for measuring pressure differences. With this size of tubing no meniscus difficulties were encountered. Water levels in the tubes were read with a cathetometer against a scale set between the manometer tubes. The scale was graduated in millimeters, and tenths of millimeters were estimated. To damp out excessive oscillations at the higher velocities, capillary tubes of 1-mm bore, about 6 inches long, were connected into the pressure lines. The damping was adjusted so that the oscillations were never completely eliminated.

Each piezometer connection at the pipes consisted of four holes, 4 mm in diameter, drilled at 90° intervals in the circumference. These were connected to a manifold and, through a valve, to the header leading to the manometer. Valves and drains were provided for flushing air from all pressure lines. It will be noted from the diagram in figure 3 that in most cases the pressure difference between two adjacent piezometers on the pipe was obtainable only by taking the difference of two readings. For example, to obtain the pressure difference between piezometers 5 and 6, it was necessary to subtract the measured difference between 1 and 5 from that between 1 and 6.

Water was supplied from a constant-level tank through a stilling tank and several lengths of straight pipe upstream from the first piezometer connection. The flow was controlled by a valve at the discharge end of the line.

The discharge was caught and measured in weighing tanks. Times were measured by stop watch. The time intervals and amounts weighed were adjusted according to the flow to obtain a minimum precision of 1 part in 2000. There was no difficulty in holding the flow constant to 1 part in 1000.

Temperatures were measured to the nearest tenth of a degree centigrade by a calibrated mercury thermometer set into the pipe near the discharge end.

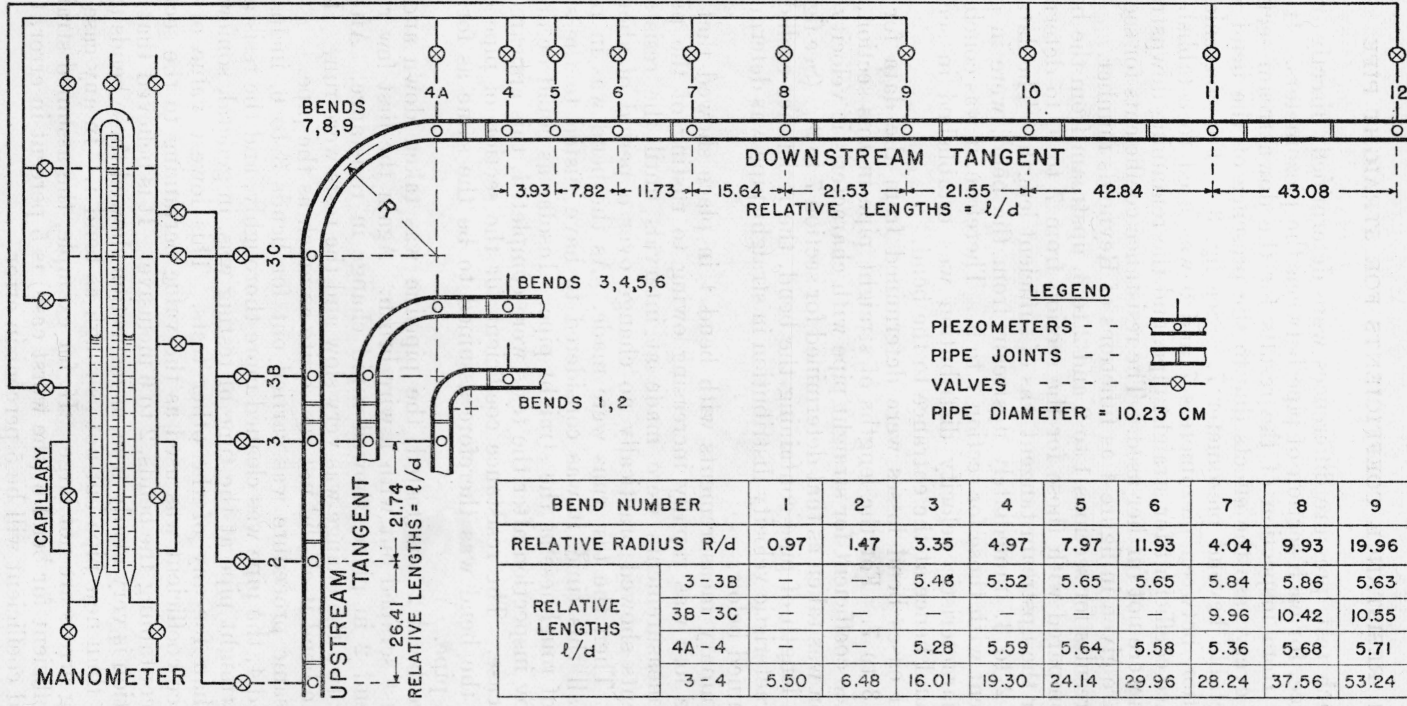


FIGURE 3.—Diagram of pipe and bend as set up for testing, showing location of pipe joints, piezometers, and arrangement of pressure connections to manometer.

IV. EXPERIMENTAL RESULTS

1. RESISTANCE COEFFICIENTS FOR STRAIGHT PIPE

In each test, pressure differences were determined, directly or by difference, for each section of pipe between the piezometers. It was evident from inspection of the results for the downstream sections that in every case the effects due to the presence of the bend were undetectable beyond piezometer 7. (See fig. 3.) For convenience, the section between piezometers 7 and 9 was used to establish the resistance coefficient for straight pipe, and the remaining downstream sections were not further used. The resistance coefficients for section 7 to 9 are given in figure 4 as functions of Reynolds number.

The results for sections 1 to 2 and 2 to 3, upstream from the bend, were compared with those for the section from 7 to 9, to determine whether the upstream tangent was of sufficient length. The data for section 2 to 3, immediately upstream from the bend, were in good agreement with those for section 7 to 9. Therefore, it was concluded that characteristic velocity distribution was established in section 2 to 3, and hence at the entrance to the bend.

In all cases bend losses were determined from the data for the section 3 to 7. For the lengths of straight pipe in this section, the resistance coefficient for straight pipe with characteristic velocity distribution was taken as that determined for section 7 to 9. (See fig. 4.) For the length of pipe containing the bend, the resistance coefficient for characteristic velocity distribution in straight pipe was determined as explained below.

Preliminary measurements with bend 1 in place showed that the pressure loss was rapidly increasing owing to rusting of the pipes. Check measurements were made at intervals until the resistance coefficients showed practically no change over a period of about 2 weeks. Then the test runs were made. As the bend was in place during all this time, it was considered to have rusted to the same degree of roughness as the straight pipe. Insofar as could be determined by inspection after the tests were completed, this appeared to be the case. The resistance coefficient for the section of pipe containing the bend was therefore assumed to be the same as for the straight pipe.

Before bend 2 was tested, the pipeline was taken down and all loose rust scraped out with a wire brush. Again the first few runs, with bend 2 in place, showed rapid change in resistance. After a week or two the change was very slow and the tests were run. However, the bend itself did not rust quite as much as the pipe.

The same procedure was carried out for bends 3 to 6, inclusive. For bend 4, the pipe was cleaned more thoroughly, and the resistance of the straight pipe at the time of testing was, in general, somewhat lower than for any of the other tests. This lowest value of the resistance coefficient was used as the value pertaining to the section of pipe containing the bends, 2 to 6 inclusive. It is believed that this assumption is very nearly true, as inspection showed these bends to be rougher than new pipe but not as rough as bend 1. In any case the resulting errors are not large. If, for example, the assumed straight pipe coefficient for bend 6 (the worst case) is 5 percent in error, then the bend coefficient will be 5 percent in error.

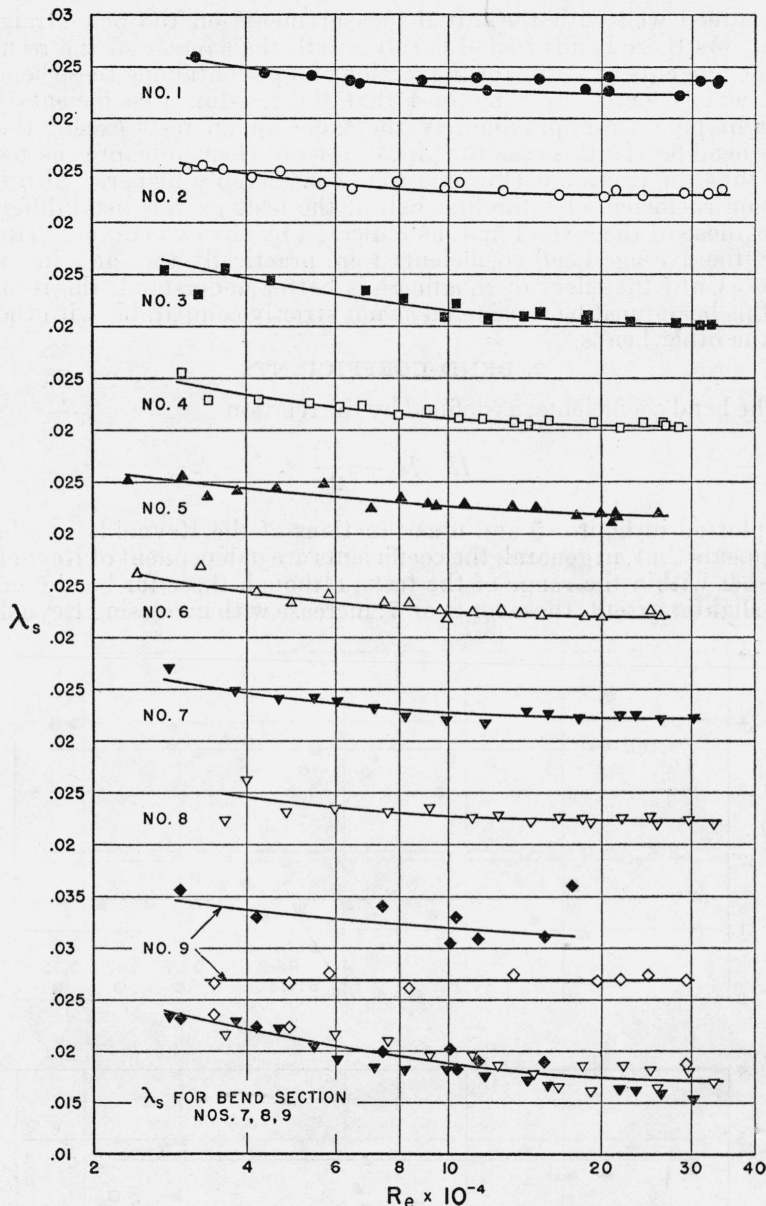


FIGURE 4.—Resistance coefficients for straight pipe as functions of Reynolds number.

The numbered curves give the resistance coefficients found in the pipe section between piezometers 7 and 9 during tests on the bends of corresponding number. The two curves for No. 9 correspond to the two groups of tests on this bend. The lowest curve represents the resistance coefficients found for the short integral upstream tangents on bends 7, 8, and 9.

The purpose of the long integral tangents on bends 7, 8, and 9 was to provide for an independent measurement of the resistance coefficient in these bends. The results, given by the lowest curve in figure 4, were rather rough on account of the relatively short lengths available,

but agreed well with the initial measurements on the new straight pipe. As these bends rusted hardly at all, the average of the results on the tangents was used for the section of pipe containing these bends.

It will be noted from figure 4 that the resistance coefficients for straight pipe are approximately the same for all tests except those with bend 9. In this case the pipes were not cleaned before the tests and thus the friction coefficients were considerably higher. Also the friction coefficients for the first half of the tests on this bend differed from those of the second half, as indicated by the two curves. However, the average bend coefficients were practically the same in each case. Until the effect of roughness is better understood, the results for this bend must be considered as not strictly comparable with those for the other bends.

2. BEND COEFFICIENTS

The bend coefficients, as defined by the relation

$$H = H_s + \eta \frac{U^2}{2g} \quad (6)$$

are plotted in figures 5 and 6 as functions of the Reynolds number. It appears that, in general, the coefficients are independent of Reynolds number within the range of the tests, although those for bend 6 and, to a slighter extent, those for bend 7, increase with increasing Reynolds

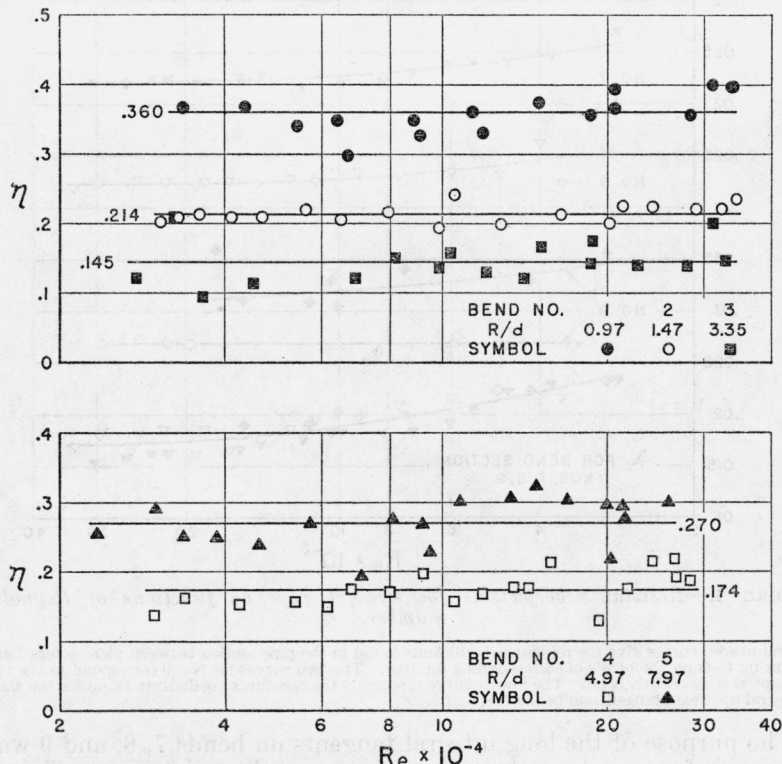


FIGURE 5.—Bend coefficients as functions of Reynolds number.

See also figure 6.

numbers. However, since the increase may very likely be due to experimental errors, the average values indicated in the figures by the heavy horizontal lines are taken to represent the results.

The average values are listed in table 1 and are plotted in figure 7 as a function of the relative radius of the bends. The *relative radius* is the ratio of the bend radius, R , to the pipe diameter, d . With the

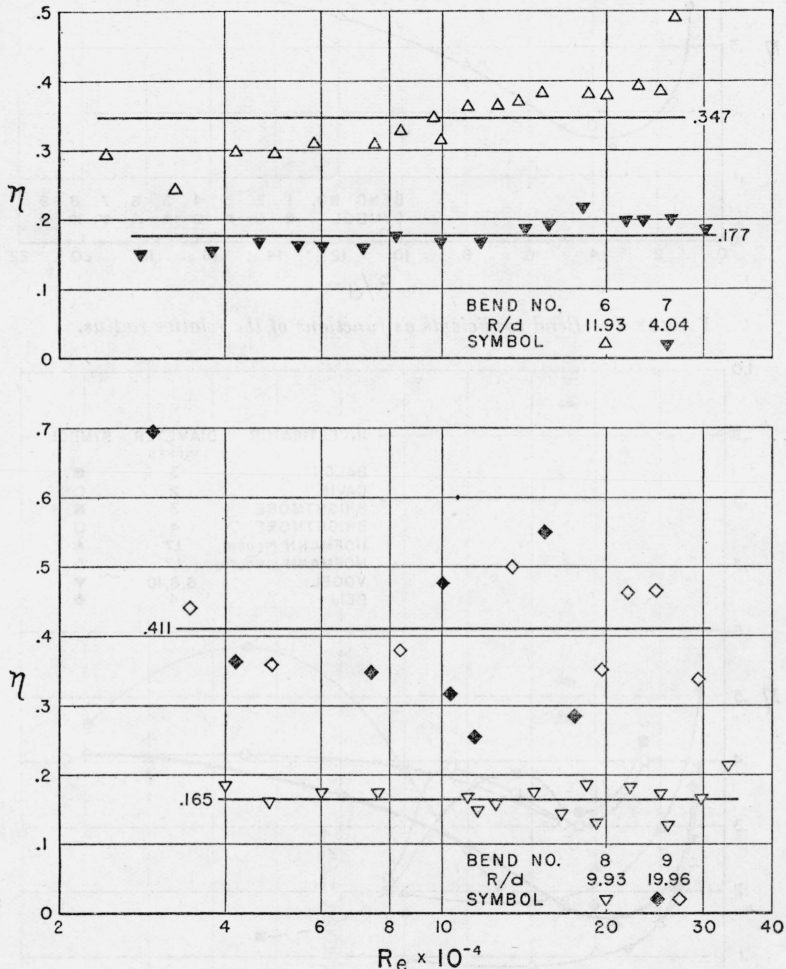


FIGURE 6.—Bend coefficients as functions of Reynolds number.

See also figure 5.

exception of the value for bend 8, the points are well represented by the smooth curve drawn in the figure. The reasons for ignoring the value for bend 8 in drawing the curve will be given later.

In figure 8, the heavy line represents the curve of figure 7, and the other curves the results of Hofmann [2], Davis [3], Balch [4], Vogel [5], and Brightmore [6]. It is evident that the quantitative agreement is not good. Even with due allowance for experimental errors (which are bound to be large from the nature of the problem), it

appears that variables other than Reynolds number and relative radius are entering.

Qualitatively there is some agreement in that the curves indicate

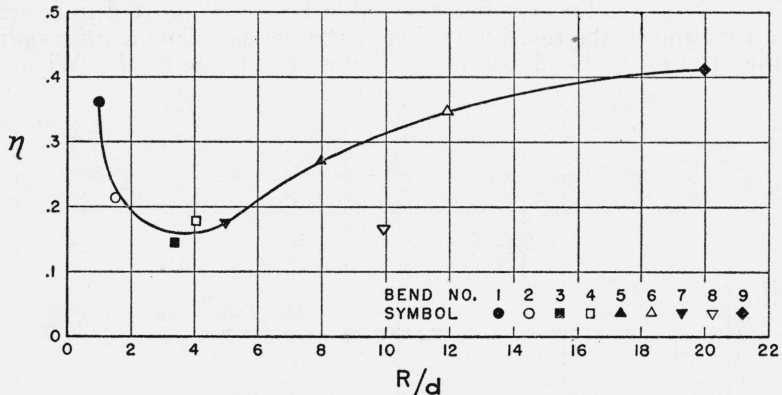


FIGURE 7.—Bend coefficients as functions of the relative radius.

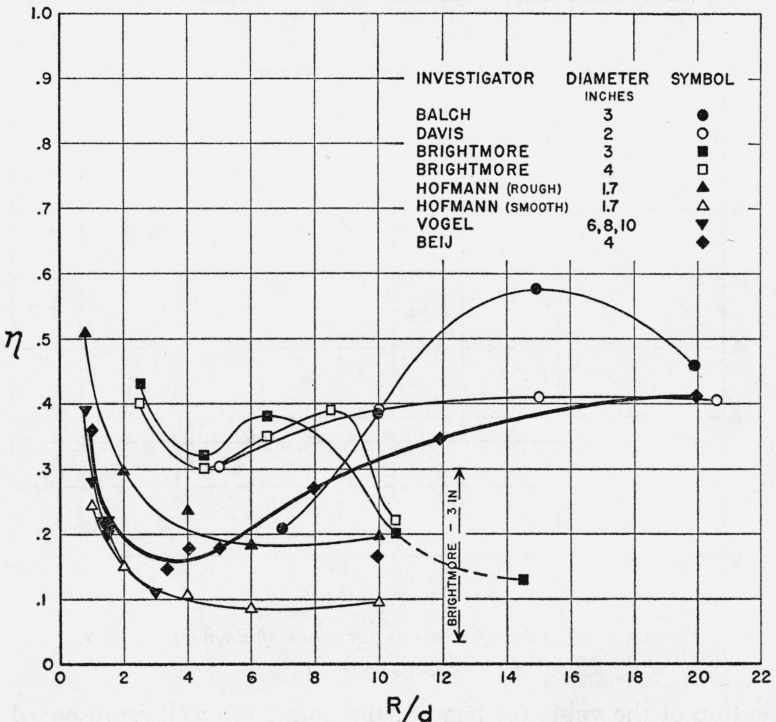


FIGURE 8.—Bend coefficients found by various investigators.

The heavy curve is the curve of figure 7 representing the results of the present investigation.

two regions of flow. For the lowest relative radii the coefficient decreases rapidly to a minimum in the neighborhood of $R/d=5$. Then there is a gradual rise to an apparent maximum somewhere near the value $R/d=15$. Finally, as the relative radius gets very

large there is probably a third region in which the coefficient decreases—presumably approaching zero as the relative radius approaches infinity.

TABLE 1.—Results of tests on 90° pipe bends—4-inch steel pipe

[Actual inside diameter, $d=10.23$ cm]

Bend	Relative radius R/d	Bend coefficient η	$(\lambda_0 - \lambda_s)$	$\frac{1}{\alpha}$	$\frac{1}{\beta}$	Tangent coefficient θ	Deflection coefficient ξ
1	0.97	0.360	0.0155	32	32	0.18	0.18
2	1.47	.214	.0155	32	32	.18	.03
3	3.35	.145	.0155	32	32	.18	-.03
4	4.97	.174	.0155	32	32	.18	-.01
5	7.97	.270	.0155	32	32	.18	.09
6	11.93	.347	.008	32	32	.09	.26
7	4.04	.178	.0155	32	32	.18	.00
8	9.93	.165	.008	32	32	.09	.08
9	19.96	.411	.0155	32	32	.18	.23

3. TANGENT COEFFICIENTS

The tangent coefficient is defined by the relation

$$H_T = \theta \frac{U^2}{2g}, \quad (3)$$

where H_T is the difference between the total head loss in the tangent and the head loss which would occur in an equal length of straight pipe with characteristic velocity distribution. Ideally, the head loss should be measured between the downstream end of the bend and some point on the tangent slightly downstream from the point where effects of the bend have disappeared. This was attempted, but it was found that accurate pressures could not be measured at the downstream end of the bend. It is believed that the disturbed flow and the rusting near or at the piezometer openings were the causes of the inconsistent pressure indications. In general, however, the measurements at piezometer 4 (fig. 3) appeared to be reliable except for a few cases. Hence, the available data consist of the head losses for the three tangent sections 4 to 5, 5 to 6, and 6 to 7, respectively.

For any point of the tangent we define a resistance coefficient λ_z by the relation

$$\frac{dh}{dz} = \lambda_z \frac{1}{d} \frac{U^2}{2g}, \quad (8)$$

where dh/dz is the head-loss gradient along the tangent and z is measured downstream from the end of the bend.

Then for a tangent section between the points $z=a$ and $z=b$, we have by integration of eq 8

$$H_{ab} = h_a - h_b = \bar{\lambda}_z \left(\frac{b-a}{d} \right) \frac{U^2}{2g}, \quad (9)$$

where $\bar{\lambda}_z$ is the mean resistance coefficient for the section. This mean coefficient was computed from the experimental data for each of the

three sections of the downstream tangent for each bend. The results showed no variation with Reynolds number, within the limits of experimental accuracy.

From these experimentally determined mean coefficients it is necessary to derive λ_z as a function of z . This function may then be integrated for the complete tangent in order to arrive at values of the excess head loss, H_T , and the tangent coefficient, θ . As the precision of the measurements is not great, a first approximation fulfilling the following conditions will suffice:

1. The function $\lambda_z = f(z)$ must agree with the experimental results for the mean coefficients λ_z .

2. The function must start at some maximum value λ_0 at the end of the bend where $z=0$, and decrease continuously, approaching

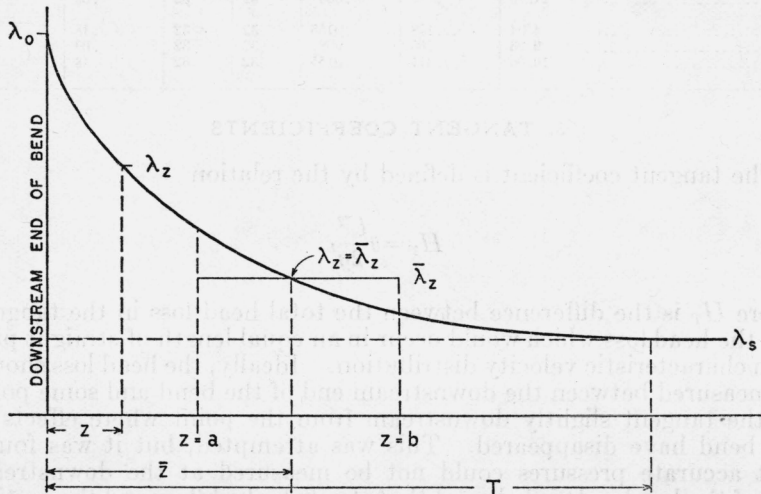


FIGURE 9.—Diagram showing the resistance coefficient in the downstream tangent as a function of the distance from the downstream end of the bend.

λ_s at $z=T$, where T does not differ greatly from the distance from the bend to the piezometer connection 7.

3. The slope of the function at $z=T$ should be very small, approaching zero.

These conditions are represented graphically in figure 9.

For the first trial the function was assumed to be

$$(\lambda_z - \lambda_s) = (\lambda_0 - \lambda_s) e^{-\alpha z/d}, \quad (10)$$

where λ_0 and α are to be evaluated from the data.

From eq 10 we may write

$$(\bar{\lambda}_z - \lambda_s) = (\lambda_0 - \lambda_s) e^{-\alpha \bar{z}/d} \quad (11)$$

where $\bar{\lambda}_z$ is the mean coefficient over the interval from $z=a$ to $z=b$, and \bar{z} is the abscissa of the point on the λ_z curve where $\lambda_z = \bar{\lambda}_z$. These relations are shown in figure 9.

Now if the section $z=a$ to $z=b$ is chosen sufficiently short, as was planned in the layout of the experiments, the value of \bar{z} will not differ

appreciably from the mean abscissa $(b-a)/2$. Hence by plotting $\bar{\lambda}_z$ as a function of $(b-a)/2$, it is possible to determine approximate values for both λ_0 and α . When this was done, it was found impossible to fulfill the conditions set up; that is, the value of λ_z at piezometer 7 was impossibly large. Hence for a second trial the function was assumed to be

$$^*(\lambda_z - \lambda_s) = (\lambda_0 - \lambda_s) e^{-\alpha z/d} \left(1 - \beta \frac{z}{d}\right) \quad (12)$$

Now $(\lambda_z - \lambda_s) = 0$ when $z = T$, and T is approximately equal to the value of z/d for piezometer 7. Hence to make the right-hand member of eq 12 vanish, we may set $1/\beta = T$ and thus obtain an approximate value of β . Using this value of β , λ_0 and α may be found as before by plotting. The final adopted values for $(\lambda_0 - \lambda_s)$, α and β are given

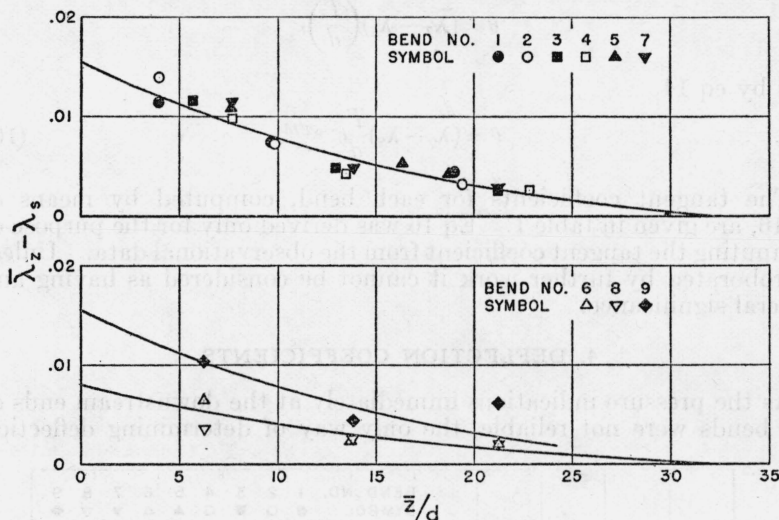


FIGURE 10.—Experimental results for the resistance coefficient in the downstream tangent as a function of the distance from the downstream end of the bend.

in table 1. It will be noticed that α equals β in every case. Thus eq 12 becomes

$$(\lambda_z - \lambda_s) = (\lambda_0 - \lambda_s) e^{-\alpha z/d} \left(1 - \alpha \frac{z}{d}\right), \quad (13)$$

where α has the value $1/32$. Finally, from this equation values of z/d for each tangent section for each bend were computed by successive approximations.

In figure 10 the experimental values of $(\lambda_z - \lambda_s)$ are plotted as functions of z/d , and the curves represent eq 13 with the values of $(\lambda_0 - \lambda_s)$ and α given in table 1. The data for bends 6, 8, and 9 are plotted separately in figure 10 since the results for these bends were erratic and the average values may be considerably in error.

By integration of eq 13 between the limits $z=0$ and $z=T$, we find

$$(\bar{\lambda}_T - \lambda_S) = (\lambda_0 - \lambda_S) e^{-\alpha T/d}, \quad (14)$$

where T is the value of z for piezometer 7. Here $\bar{\lambda}_T$ is the mean resistance coefficient for the whole tangent.

But we may write

$$H_T = (\bar{\lambda}_T - \lambda_S) \left(\frac{T}{d} \right) \frac{U^2}{2g}, \quad (15)$$

and this relation combined with

$$H_T = \theta \frac{U^2}{2g} \quad (3)$$

gives for the tangent coefficient

$$\theta = (\bar{\lambda}_T - \lambda_S) \left(\frac{T}{d} \right),$$

and by eq 14,

$$\theta = (\lambda_0 - \lambda_S) \frac{T}{d} e^{-\alpha T/d}. \quad (16)$$

The tangent coefficients for each bend, computed by means of eq 16, are given in table 1. Eq 16 was derived only for the purpose of computing the tangent coefficient from the observational data. Unless corroborated by further work it cannot be considered as having any general significance.

4. DEFLECTION COEFFICIENTS

As the pressure indications immediately at the downstream ends of the bends were not reliable, the only way of determining deflection

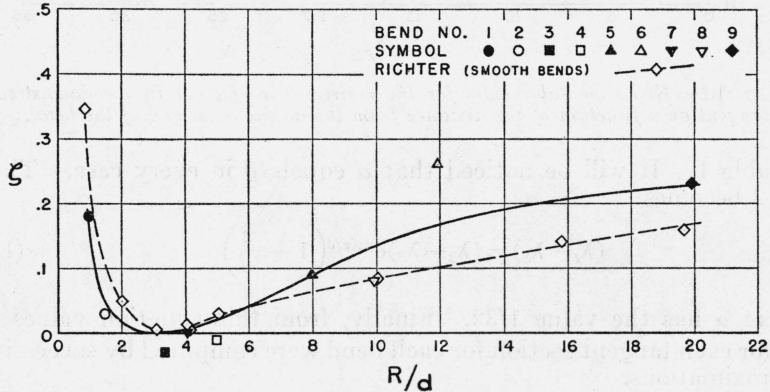


FIGURE 11.—Deflection coefficients as functions of the relative radius.

Richter's results for smooth bends are given for comparison.

coefficients was to evaluate the tangent coefficient as in the preceding section and then find ξ from the relation

$$\eta = \xi + \theta. \quad (7)$$

The results are given in table 1 and in figure 11 where ξ is plotted as a function of the relative radius. Since the tangent coefficients for bends 6, 8, and 9 are possibly subject to large errors, the deflection coefficients for these bends are also open to question. In figure 11, there are also plotted for comparison the values of ξ obtained for smooth pipe by direct measurements by Richter [7].

V. DISCUSSION OF RESULTS

1. RUSTING OF PIPES

The great disadvantage of ferrous pipes for hydraulic experiments is their progressive rusting which results in a continually changing roughness. With care in manipulation, and with unlimited time for the work, it is possible to obtain average resistance coefficients for straight pipes varying not more than about 5 percent from the mean. However, there can be no assurance that the resistance coefficient is the same at all points in the line. The difficulties are increased when dealing with bends, for it is not possible to make determinations of the friction coefficients after a pipe has been bent. The worst effect of rusting, however, appears at the piezometer holes. Here ridges of rust are frequently built up around the holes in such a way as to falsify the pressure indications.

Thus, regardless of the relative magnitude of roughness effects, for a final solution of the bend problem it will be necessary to deal first with smooth pipes and then with pipes of known and unvarying roughness; that is, with pipes artificially roughened. A start in this direction has been made by Hofmann [2].

2. PIPE JOINTS

Very probably some of the discrepancies between results of different observers may be laid to extraneous factors, such as irregular pipe joints, which should properly be excluded in tests of bends. In most of the recent work great care has been taken to set up practically jointless pipe lines as, for example, in Hofmann's and Richter's work and in the work herein reported. However, in some instances the opposite has been the case, the desire being to experiment on pipe lines similar to those in actual practical use. The total effect of irregular joints may become quite appreciable even though the joints appear to be well made. In some unpublished tests of straight 4-inch galvanized pipe with screwed couplings, made at the time of the bend tests, the resistance coefficient was increased 10 percent or more by joints at 10-foot intervals.

3. BEND COEFFICIENT

The results presented in figure 8 show clearly the two flow regimes in 90° pipe bends. For very sharp bends, the bend coefficient drops rapidly to a minimum as the relative radius increases to a value in the neighborhood of $R/d=5$. As the relative radius is still further increased to a value of $R/d=20$, the results of each investigator appear to follow a definite relationship, but no two investigators find the same relationship.

Hofmann's data (fig. 8) apparently establish the fact that roughness is an important factor for bends of relative radius less than $R/d=10$. If this is so, and granting that all the data shown in figure 8 are correct, then it should be possible to establish a relation between the various curves representing the results of the different investigators and the relative roughness of the pipes. For rough pipes we have the relations [8]

$$\frac{U}{u_*} = 8.12 \left(\frac{r}{2k} \right)^{1/6}, \text{ and}$$

$$\frac{U}{u_*} = \sqrt{\frac{8}{\lambda}},$$

where

u_* = the shear velocity,

k = the absolute roughness, and

r = the radius of the pipe.

Combination of the two relations gives

$$\frac{k}{r} = 280 \lambda^3.$$

From this relation and the published data, values of the relative roughness were computed or estimated. Then the bend coefficients from the curves in figure 8 were plotted against the corresponding relative roughness, as shown in figure 12. For smooth pipe (Hofmann's data) the relative roughness was taken as zero.

While the procedure may not be entirely free from objection, the results in figure 12 are sufficiently suggestive to warrant further work in this direction. It should be stated that Brightmore's data for 3-inch bends have been omitted from figure 12. In these tests he used cast iron bends with galvanized iron pipe tangents. Thus there was no logical procedure for calculating the effective relative roughness.

Conceivably roughness may affect the bend coefficient in three ways. First, the velocity distribution at the entrance to the bend will depend on the roughness of the upstream tangent. Second, the shear at the wall in the bend itself will vary according to the roughness. Third, and probably most important, the excess loss in the downstream tangent will be dependent on roughness. From figure 11 it would appear that roughness has little or no effect on the bend coefficient when the relative radius is less than 6. Hence the greater part of the roughness effect shown in figure 12 must be localized in the downstream tangent. However, further work is necessary before final conclusions can be drawn.

At first sight it does not appear possible to draw any general conclusions from the results in figure 8 for the range of relative radius from $R/d=5$ to $R/d=20$. The following points should be noted, however.

1. The curves representing the data of Davis and of Balch rise from a low value of $R/d=5$ to 7 to a maximum at about $R/d=15$ and then begin to decrease.

2. Hofmann's values indicate the beginning of a much more gradual rise with correspondingly lower values of the bend coefficient.

3. Brightmore's curves start to rise but suddenly drop to low values in the neighborhood of those found by Hofmann.

4. There are two significant irregularities. For a 3-inch bend with $R/d=12$, Brightmore was unable to obtain consistent results. The extreme values are indicated in the figure by the arrows. He states, "in the case of the 3-inch bend with radius equal to 12 diameters, for velocities exceeding 3 feet per second the flow becomes unstable, the loss of head sometimes being much smaller than would be inferred from the losses in the bends of radii equal to 10 and 14 diameters respectively." Also in the present investigation the bend coefficient for bend 8 of relative radius equal to 10 was unexpectedly low. The value obtained is indicated in figure 8 by the isolated point.

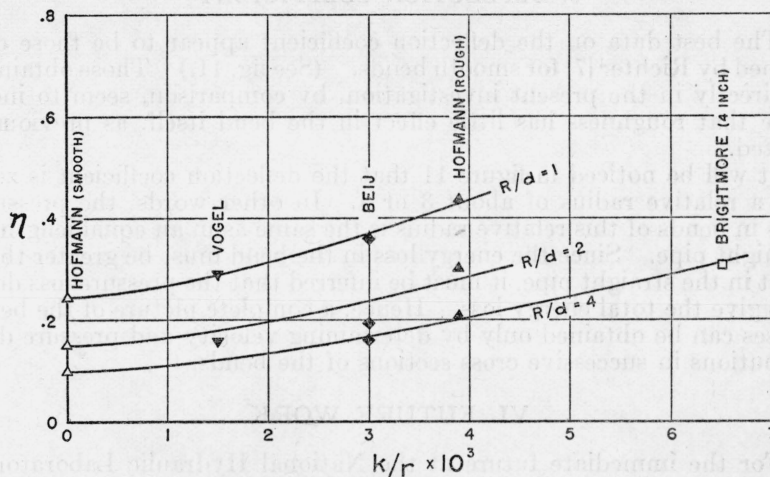


FIGURE 12.—Bend coefficients for bends of small relative radii determined by various investigators as functions of the relative roughness.

From the foregoing observations, it may be concluded that in the range from $R/d=5$ to $R/d=15$ or 20 the bend coefficient is not a function of the flow, the relative radius, and the roughness only. Some other variable or variables enter which produce what appears to be a sort of instability manifested by the wide range in results obtained by different or the same observer, and in one case by the very irregular results obtained by one observer for one particular bend. If the explanation is to be found, as seems likely, in relatively small disturbances of entrance conditions, or small geometrical irregularities, then for engineering purposes a curve of maximum values should be established. For this reason the curve in figure 7 was drawn through the highest points.

For bends of relative radii greater than 20 (or perhaps a somewhat larger value) it would seem that the bend coefficient should decrease asymptotically toward zero. While of little importance from the engineering standpoint, this range of relative radii should be explored as the results will very likely be helpful in the solution of the general problem.

4. TANGENT COEFFICIENT

One interesting fact relative to the resistance in the downstream tangent is disclosed by the present investigation. That is, for bends of relative radii less than $R/d=8$, the excess pressure loss in the tangent and the apparent resistance coefficient, λ_0 , at the downstream end of the bend are independent of the relative radius. This conclusion is derived from the results plotted on the upper graph of figure 10. This graph shows that the resistance coefficients, and hence the losses, are the same for all six bends of relative radius less than 8. Here again, more precise data covering a wider range of conditions are essential for clearing up the many uncertainties.

5. DEFLECTION COEFFICIENT

The best data on the deflection coefficient appear to be those obtained by Richter [7] for smooth bends. (See fig. 11.) Those obtained indirectly in the present investigation, by comparison, seem to indicate that roughness has little effect in the bend itself, as previously stated.

It will be noticed in figure 11 that the deflection coefficient is zero for a relative radius of about 3 or 4. In other words, the pressure loss in bends of this relative radius is the same as in an equal length of straight pipe. Since the energy loss in the bend must be greater than that in the straight pipe, it must be inferred that the pressure loss does not give the total energy loss. Hence, a complete picture of the bend losses can be obtained only by determining velocity and pressure distributions in successive cross sections of the bends.

VI. FUTURE WORK

For the immediate future at the National Hydraulic Laboratory, work on flow in bends will be limited to smooth pipes and bends. Tests are already under way on coils of relatively low R/d values, and it is hoped that these will be followed by studies of very long bends at large values of R/d .

VII. REFERENCES

- [1] G. H. Keulegan and K. H. Beij, *Pressure losses for fluid flow in curved pipes*, J. Research NBS **18**, 89 (1937) RP965.
- [2] A. Hofmann, *Der Verlust in 90°-Rohrkrümmern mit gleichbleibendem Kreisquerschnitt*, Doc. Thesis, Tech. Hoch. München, (R. Oldenbourg, München, 1929). Also in Mitt. Hydr. Inst. Tech. Hoch. München, Heft 3 (1929).
- [3] G. J. Davis, *Investigation of Hydraulic Curve Resistance*, Univ. Wisc. Bul. 403, Eng. Series 6, 115 (1911).
- [4] L. R. Balch, *Investigation of Hydraulic Curve Resistance, Experiments with Three-Inch Pipe*, Univ. Wisc. Bul. 578, Eng. Series 7, 253 (1913).
- [5] H. D. Vogel, *Head Losses in Various Types of Pipe Bends*, U. S. Waterways Exp. Sta. Pap. HS, Limited edition series (1933).
- [6] A. W. Brightmore, *Loss of pressure in water flowing through straight and curved pipes*, Min. Proc. Inst. Civil Engrs. **169**, 315 (1906-07).
- [7] H. Richter, *Der Druckabfall in gekrümmten glatten Rohrleitungen*, Forsch. Arb. Geb. Ing. **338** (1930).
- [8] G. H. Keulegan (unpublished work).

WASHINGTON, April 11, 1938.